ABSTRACT

PROPERTIES OF GAMMA-RAY TRANSITIONS IN ^{56}Co
FROM ^{56}Ni DECAY AND ^{56}Fe(p,$n\gamma$)^{56}Co

By

Lawrence Edward Samuelson

The ^{56}Ni beta decay and the ^{56}Fe(p,$n\gamma$)^{56}Co reaction with beam energies between 5.5 and 8.4 MeV have been used with Ge(Li) spectrometers to study properties of γ rays from states of ^{56}Co below 2.85 MeV of excitation. The ^{56}Ni decay γ-ray spectrum and γ-γ coincidences were studied. γ-γ coincidences, γ-ray excitation functions, γ-ray angular distributions, and absolute cross sections were measured for the ^{56}Fe(p,$n\gamma$)^{56}Co reaction. A beta-decay scheme for ^{56}Ni, which includes six γ rays, and an energy-level diagram for ^{56}Co, which includes 35 γ rays (14 of which are reported for the first time) from 20 excited states, are presented. Comparisons of the data from ^{56}Fe(p,$n\gamma$)^{56}Co with predictions of the statistical compound nuclear model have resulted in spin assignments (in parentheses) for the following states (energies in keV) of ^{56}Co: 158.4 (3), 576.6 (5), 829.7 (4), 970.3 (2), 1009.2 (5), 1114.6 (3), 1450.8 (0), and 1720.3 (1). Branching ratios are presented for 14 γ rays from these eight states and multipole mixing ratios are given for 12 of these γ rays (10 are predominantly M1). The data are consistent with a

spin 4 assignment to the ground state. Contrary to previous suggestions, evidence from all experiments indicates that only one state exists in ^{56}Co in the neighborhood of 1451 keV of excitation. The level energies, γ-ray multipole mixing ratios and γ-ray branching ratios agree, in general, with shell-model predictions of McGrory.

PROPERTIES OF GAMMA-RAY TRANSITIONS IN ^{56}Co FROM ^{56}Ni DECAY AND $^{56}Fe(p,n\gamma)^{56}Co$

By

Lawrence Edward Samuelson

A THESIS

Submitted to
Michigan State University
in partial fulfillment of the requirements
for the degree of

DOCTOR OF PHILOSOPHY

Department of Physics

1972

ACKNOWLEDGMENTS

I wish to thank Dr. W. H. Kelly for suggesting this area of study. His encouragement and constant interest during the experimental work and his guidance and patience during the preparation of this thesis are deeply appreciated.

I also wish to thank most sincerely Dr. R. A. Warner for his invaluable assistance and encouragement in all phases of this work. Many fruitful discussions led to solutions of apparently insurmountable problems.

Drs. Wm. C. McHarris, F. M. Bernthal and B. H. Wildenthal have contributed to various phases of this investigation through informal discussion. Dr. J. B. McGrory was very kind to send shell-model calculations on ^{56}Co. Their generous cooperation is gratefully acknowledged.

Dr. H. G. Blosser and Mr. H. Hilbert have assisted with the operation of the Michigan State University sector-focused cyclotron.

Dr. E. M. Bernstein, Dr. R. Shamu and Mr. Eric Warren assisted considerably with the operation of the Western Michigan University tandem Van de Graaff. Their unselfish generosity is gratefully appreciated.

Dr. R. E. Doebler, Dr. R. R. Todd, Dr. R. W. Goles, Mr. C. B. Morgan and Mr. W. B. Chaffee aided in data collection and interpretation.

Mrs. Carol VanderMeer and Mrs. Peri-Anne Warstler aided greatly by typing the various versions of this manuscript.

Much of the financial assistance for this research has been provided by the National Science Foundation, the U.S. Atomic Energy Commission, and Michigan State University.

TABLE OF CONTENTS

		Page
ACKNOWLEDGMENTS		ii
LIST OF TABLES		v
LIST OF FIGURES		vii
I.	INTRODUCTION	1
II.	THE BETA DECAY OF ^{56}Ni	3
	A. Source Preparation	3
	B. The γ-ray Spectrum	4
	C. γ-γ Coincidences	8
	D. The ^{56}Ni Beta-Decay Scheme	12
III.	THE ^{56}Fe$(p,n\gamma)^{56}$Co REACTION	16
	A. γ-γ Coincidences	18
	B. γ-ray Excitation Functions	32
	C. γ-ray Angular Distributions	46
	D. Total Absolute Cross Sections at E_p=7.30 MeV	61
IV.	DISCUSSIONS OF INDIVIDUAL LEVELS	65
	A. Ground State, $J^\pi=4^+$	65
	B. E_x=158.4 keV, 3^+	66
	C. E_x=576.6 keV, 5^+	67
	D. E_x=829.7 keV, 4^+	67
	E. E_x=970.3 keV, 2^+	69
	F. E_x=1009.2 keV, 5^+	69
	G. E_x=1114.6 keV, 3^+	70
	H. E_x=1450.8 keV, 0^+	71
	I. E_x=1720.3 keV, 1^+	74
	J. Higher Excited States	77

Page

V. COMPARISONS WITH SHELL MODEL CALCULATIONS FOR ^{56}Co. 79

VI. SUMMARY AND CONCLUSIONS 88

BIBLIOGRAPHY. 91

APPENDICES. 96

A. Separation of Nickel from Irradiated Iron Shimstock. 96

B. Integral Coincidence and Gated Spectra from the ^{56}Fe(p,$n\gamma$-γ)^{56}Co Reaction at E_p=7.38 and 8.36 MeV. . 97

C. γ-ray Angular Distributions from the ^{56}Fe(p,$n\gamma$)^{56}Co Reaction at E_p=5.77, 6.65, 7.03, 7.05, 7.30, and 7.40 MeV 106

D. The Experimental and Theoretical Values of the A_2^* and A_4^* ^{56}Co γ-ray Angular Distribution Coefficients as a Function of the γ-ray Mixing Ratio δ 120

E. Relative χ^2 as a Function of Arctan δ for the ^{56}Co γ-ray Angular Distributions 130

LIST OF TABLES

Table — Page

I. Energies and relative intensities of the γ rays in ^{56}Co from the beta decay of ^{56}Ni. 7

II. Summary of two-parameter γ–γ coincidence results for the ^{56}Ni $\overset{\varepsilon}{\rightarrow}$ ^{56}Co decay. 11

III. Energies of γ rays found in ^{56}Co at excitations up to 2.86 MeV from ^{56}Fe$(p,n\gamma)^{56}$Co. Unless otherwise indicated, the identification of ^{56}Co γ rays are based upon both γ-ray excitation functions and γ–γ coincidences 24

IV. Results of two parameter γ–γ coincidence experiments from ^{56}Fe$(p,n\gamma\text{-}\gamma)^{56}$Co. 25

V. γ-ray energy standards used as calibrations in the determination of ^{56}Co γ-ray energies from ^{56}Fe$(p,n\gamma)^{56}$Co. Those γ rays listed for the isotope ^{56}Fe appeared in the spectra from ^{56}Fe$(p,p'\gamma)$. 27

VI. Form of the optical-model potential and parameters used in the calculations of transmission coefficients. The Coulomb potential, $V_c(r)$, is that due to a uniformly charged sphere of radius $1.25A^{1/3}$ [F]. The parameter E is the center-of-mass energy of the nucleon in MeV. 43

VII. Experimental γ-ray angular distribution fitting parameters A_2^* and A_4^* and the associated γ-ray

Table

Page

multipole mixing ratio, δ. The fitting parameters and mixing ratio are defined in the text. The errors assigned to both the A_2^* and A_4^* coefficients represent plus or minus one standard deviation. The ranges of δ were determined from these coefficients as described in the text 53

VIII. $^{56}Fe(p,n)^{56}Co$ total cross sections at E_p = 7.30 MeV. 63

IX. Reduced transition probabilities, B(M1) and B(E2), calculated by McGrory[a] and comparisons of the shell-model results with experimental γ-ray multipole mixing ratios, δ, and γ-ray branching ratios from $^{56}Fe(p,n\gamma)^{56}Co$. The experimental transition energies were used when calculating the theoretical mixing and branching ratios (necessary formulas are presented in the text).. 83

X. Shell-model predictions by McGrory[a] of the half lives of the first eight excited states of ^{56}Co. Only observed transitions were included in these calculations. Internal-conversion effects were not included 85

LIST OF FIGURES

Figure		Page
1.	Typical ^{56}Ni singles spectrum taken with the 2.5%-efficient Ge(Li) spectrometer	5
2.	Integral coincidence and gated spectra from the ^{56}Ni γ-γ coincidence experiment. Peaks labeled with a Σ were identified as triple coincidences where two of the three coincident γ rays have been summed in one detector. Peaks labeled in parentheses are believed to be from chance coincidences or insufficient background subtraction.	9
3.	Decay scheme of ^{56}Ni. The γ-ray energies were measured using the ^{56}Ni decay. The intensities have been rounded off and are normalized to 100 for the 158.4-keV transition strength. The ^{56}Ni decay half life and the half lives of the 158.4-, 970.2-, and 1450.7-keV states are from Ref. 1. The ^{56}Co ground-state half life is from Ref. 5. The Q_ε value is from Ref. 42. The spin and parity assignments are from ^{56}Fe$(p,n\gamma)^{56}$Co and are discussed in the text. Log ft values are also discussed in the text.	13
4.	Geometry for the in-beam γ-γ coincidence measurements. The squares are not meant to represent the actual size of the Ge(Li) detectors, but only the approximate location of their cryostat caps.	19

Figure

Page

5. Integral coincidence and representative gated spectra from the $^{56}Fe(p,n\gamma-\gamma)^{56}Co$ $\gamma-\gamma$ coincidence experiment at E_p = 8.36 MeV. γ-rays labeled with a question mark, although they appear to be in coincidence, could not be placed in the decay scheme. Peaks labeled in parenthesis are believed to be from chance coincidences or insufficient background subtraction. 21

6. The γ-ray decay scheme for excitations of ^{56}Co. The γ-ray energies and branching ratios were measured using $^{56}Fe(p,n\gamma)^{56}Co$. The arrows on the right indicate the maximum possible excitations for the proton energies of the $\gamma-\gamma$ coincidence and γ-ray angular distribution experiments. The spins, parities, and level energies labeled with an asterisk are from Ref. 15, while the remaining values were determined from $^{56}Fe(p,n\gamma)^{56}Co$. Dots denote observed coincidence relationships between γ-ray transitions entering and leaving a state 29

7. Typical γ-ray spectra from the excitation function measurements. The first appearances of the various ^{56}Co γ rays are labeled. 33

8. Excitation functions for the first eight excited states of ^{56}Co. The units of the ordinate are arbitrary but are proportional to the absolute cross section. The data were taken at 125°, a

Figure Page

zero of $P_2(\cos\theta)$, in order to minimize angular distribution effects. Neutron feedings were computed for each level from the γ-ray intensity imbalances, and then were normalized from run to run (as described in the text) to obtain the relative cross sections. The thresholds were calculated using Q = -5.357 MeV for the ground state (Ref. 48) and are connected to the first non-zero data points with dotted lines. Solid lines connect the data to guide the eye. Where not visible, error bars are smaller than the data-point symbol 36

9. Experimental and theoretical cross-section ratios. The ratios are taken with respect to the 158.4-keV first excited state. Error bars identify the data (lines connecting the data are to guide the eye). MANDY predictions for selected beam energies are shown for $J^\pi = 0^+,\ldots,6^+$. A $J^\pi = 3^+$ for the 158.4 keV state was used as explained in the text. Straight lines connecting the theoretical points approximate expected smooth curves 40

10. Geometry for the in-beam γ-ray angular distribution measurements. The monitor and target angles were held fixed throughout all of the measurements. 47

11. Angular distributions of ^{56}Co γ rays taken at E_p = 5.77, 6.65, 7.05, 7.30, and 7.40 MeV. The solid lines through the data represent least squares fits using

Figure

Page

the equation for $W(\theta)$ given in the text. $W(\theta)$ has been normalized to 1 at 90°. Except for the E_p = 7.40 MeV case, two experimental points were taken at each angle; only their weighted average is presented 51

12. Representative plot of MANDY predictions for the A_2^* and A_4^* coefficients as a function of γ-ray mixing ratio, δ. (Definitions are presented in the text.) This plot is for the case of the 158.4-keV γ ray at E_p = 5.77 MeV. A spin of 4 for the final state was assumed; the spins and parities of the initial state label their appropriate δ-ellipses. Representative values of δ are also labeled. The experimental A_2^* and A_4^* coefficients including uncertainties are shown as a rectangle in approximately the center of the plot. 55

13. Representative relative χ^2 versus arctan δ plots for angular distributions of each of the ^{56}Co γ rays. J^π values for the initial states label each curve. The J value assumed for the final state was that previously assigned in this work 58

14. Comparisons of level spins, parities, and energies of the present experiment and from Ref. 15 (asterisked values), with the predictions of McGrory (Ref. 30). Dashed lines indicate tentative correlations. For excitations above 3 MeV, see Ref. 15. 80

Figure Page

15. Integral coincidence and gated spectra from the $^{56}Fe(p,n\gamma)^{56}Co$ reaction at E_p = 7.38 and 8.36 MeV. The x-axis is from the 2.5% detector while the y-axis is from the 7.4% detector. Background subtraction using the adjacent continuum has been included. Peaks labeled in parenthesis are believed to be from chance coincidences or insufficient background subtraction. More details are given in the text. 97

16. γ-ray angular distributions from the $^{56}Fe(p,n\gamma)^{56}Co$ reaction at E_p = 5.77, 6.65, 7.03, 7.05, 7.30, and 7.40 MeV. The solid lines through the data represent least squares fits using the equation for $W(\theta)$ given in the text. $W(\theta)$ has been normalized to 1 at 90°. Except for the E_p = 7.40 MeV case, two experimental points were taken at each angle; only their weighted average is presented. The assignment of errors is outlined in the text. 106

17. Plots of the experimental and theoretical values of the A_2^* and A_4^* ^{56}Co γ-ray angular distribution coefficients as a function of γ-ray mixing ratio δ. (Definitions and descriptions for the calculations are presented in the text.) Only those cases are shown where γ-ray feeding from above was judged to be insignificant. In each case the spin used

for the final state was that determined from this experiment; the possible initial state spins and parities label their appropriate δ-ellipses. Approximate locations for the values of δ can be found by comparison with Fig. 12. In each case the 1^+ "ellipse" is a short straight vertical line passing through the point $A_2^* = 0.0$, $A_4^* = 0.0$. The experimental A_2^* and A_4^* coefficients including uncertainties are shown on each plot as a rectangle 120

18. Plots of relative χ^2 versus arctan δ for ^{56}Co γ-ray angular distributions. Only those cases are shown where γ-ray feeding from above was judged to be insignificant. Assignment of errors necessary for the determination of χ^2 is outlined in the text. In each case the spin used for the final state was that determined from this experiment; the possible initial state spins and parities label their appropriate curves. It is instructive to compare these plots with the corresponding plot of Fig. 17 130

I. INTRODUCTION

The earliest investigations[1-6] of the low-lying excited states of ^{56}Co began with the beta decay of ^{56}Ni. These studies, which included measurements of the ^{56}Ni half life,[1] the γ-ray spectrum,[1,3,4] γ-γ angular-correlations,[1,3] the internal-conversion electron spectrum,[2] and lifetimes of some ^{56}Co states,[1] produced valuable information. However, only selected states below 1.8 MeV could be populated and unambiguous spin assignments for these states could not be made.

More recently, experiments involving the two-particle transfer reactions ^{54}Fe(^{3}He,p)^{56}Co,[7-10] ^{54}Fe(α,d)^{56}Co,[11] ^{58}Ni(p,^{3}He)^{56}Co,[12] and ^{58}Ni(d,α)^{56}Co[8,9,13-15] and the charge-exchange reactions ^{56}Fe(p,n)-^{56}Co[16,17] and ^{56}Fe(^{3}He,t)^{56}Co[18-21] have increased the knowledge of the properties of these and additional states. However, the interpretations of these experiments depend strongly upon assumed ^{56}Co wave functions and reaction mechanisms. Neither is well-known.

In particular, the J^{π} of a state in ^{56}Co at 1451 keV has been somewhat controversial. In the early ^{56}Ni decay work, 1^- or $2^{\pm}$ seemed most consistent with the data, with $1^-(2^-)$ being favored by Ohnuma *et al.*,[3] and 2^+ by Jenkins *et al.*[2] and Wells.[22] Later, Belote *et al.*,[8] observing $\ell = 0$ transfers in (^{3}He,p) and (d,α) and a weak (d,α) cross section, chose 0^+. Belote *et al.*[8] then conjectured that this state was an anti-analog of the ^{56}Fe ground state ($J^{\pi} = 0^+$). Subsequent particle transfer work has confirmed $J^{\pi} = 0^+$ (e.g. see Ref. 12 and 15). However, Roos and Goodman[19] reported an $\ell = 1$ transfer in the (^{3}He,t) reaction, implying $J^{\pi} = 1^-$; they then suggested that possibly a 0^+ *and* a 1^- state occur within a few keV of each

other at this energy.

The $^{56}Fe(p,n\gamma)^{56}Co$ reaction[23,24] near threshold was chosen for the present study because the reaction should be well described by the statistical compound nuclear (CN) theories of Wolfenstein,[25] Hauser and Feshbach,[26] Biedenharn and Rose,[27] Satchler,[28] and Sheldon and Van Patter.[29] Since all states for which there are sufficient energy and angular momentum are excited in this type of reaction, both members of the doublet (if they exist) at 1451 keV should be populated quite strongly because of their expected low spins. Comparisons of the results of the present work with the predictions of the statistical CN theory and with previously measured ^{56}Co γ-ray characteristics have lead to unambiguous spin assignments for all ^{56}Co states below 1.8 MeV. In addition, γ-ray multipole mixing ratios, precise level energies and γ-ray branching ratios are obtained. This experimental information is compared with shell-model level energies and B(M1) and B(E2) values for ^{56}Co calculated recently by McGrory.[30]

As a supplement to the $(p,n\gamma)$ work, the γ-ray spectrum accompanying the ^{56}Ni beta decay was reinvestigated. These experiments corroborated the previous ^{56}Ni decay work and the energies of some ^{56}Co γ-rays. In particular, the 1451 keV state was examined very carefully in the decay study for any evidence of it being a doublet.

II. THE BETA DECAY OF ^{56}Ni

Ge(Li) detectors were used to measure the γ-ray spectrum and γ-γ coincidences accompanying the ^{56}Ni beta decay. These experiments yielded γ-ray energies and intensities and confirmed the placement of γ-rays in the ^{56}Ni decay scheme.

A. Source Preparation

The 6.1-day ^{56}Ni activities were produced via the ^{56}Fe(^{3}He,3n)^{56}Ni reaction (Q = -16.3 MeV) by bombarding 0.02 gm/cm^2 iron foils with 45-MeV ^{3}He particles from the Michigan State University sector-focused cyclotron. After allowing about 10 days for the undesired 1.5-day ^{57}Ni activity to decay, chemical separations were performed.

The iron foils were first dissolved in hot 15N HCl, evaporated to dryness, and redissolved in 10N HCl. The samples were then passed through a column of Dowex 1-X8 anion exchange resin previously brought into equilibrium with 10N HCl. This procedure[31] removed all detectable contaminant cobalt activities such as ^{56}Co and ^{58}Co. The desired ^{56}Ni activities were then separated from the remaining contaminant radioisotopes such as ^{51}Cr, ^{52}Mn, and ^{54}Mn by the standard procedure of precipitation of nickel dimethylglyoxime (Ni-DMG).[32] The Ni-DMG was finally dissolved in 15N HCl and placed in thin-walled plastic vials for counting.

B. The γ-Ray Spectrum

Three different Ge(Li) detectors were used to take γ-ray singles spectra: (1) a 2.5%-efficient (compared to a 7.6 cm × 7.6 cm NaI(Tl) detector at 25 cm and at a γ-ray energy of 1332 keV) Ge(Li) detector with a 15:1 peak-to-Compton ratio and a FWHM resolution of 2.34 keV at a γ-ray energy of 1332 keV; (2) a 4.5%-efficient Ge(Li) detector with a 22:1 peak-to-Compton ratio and a FWHM resolution of 2.10 keV; and (3) a 10.4%-efficient Ge(Li) detector with a 30:1 peak-to-Compton ratio and a FWHM resolution of 2.28 keV. A typical ^{56}Ni decay γ-ray singles spectrum is shown in Fig. 1. Optimum resolution and the most symmetric peaks were obtained using an ORTEC model #450 Research Amplifier direct-coupled into a Northern Scientific 50-MHz analog-to-digital converter. The data were accumulated in either the MSU Cyclotron Laboratory's Xerox Data System Σ-7 time-sharing computer using a pulse-height analysis routine,[33] or in a Digital Equipment Corporation PDP-9 computer loaded with another pulse-height analysis routine. Peak centroids and areas were determined off-line by the peak-fitting code SAMPO,[34] which was especially useful in stripping unresolved multiplets.

Since it offered the best over-all resolution, the 4.5%-efficient Ge(Li) detector was used to take the spectra for the γ-ray energy measurements. For these measurements, spectra from a ^{56}Ni source were taken in the presence of various combinations of such well-known γ-ray energy standards as ^{57}Co, ^{139}Ce, ^{203}Hg, ^{51}Cr, ^{207}Bi, ^{137}Cs, ^{54}Mn, ^{56}Co, ^{88}Y, ^{65}Zn, ^{60}Co, ^{22}Na, ^{40}K, and ^{192}Ir. The calibration energies assumed can be found elsewhere.[5,35,36] Care was taken so that standard

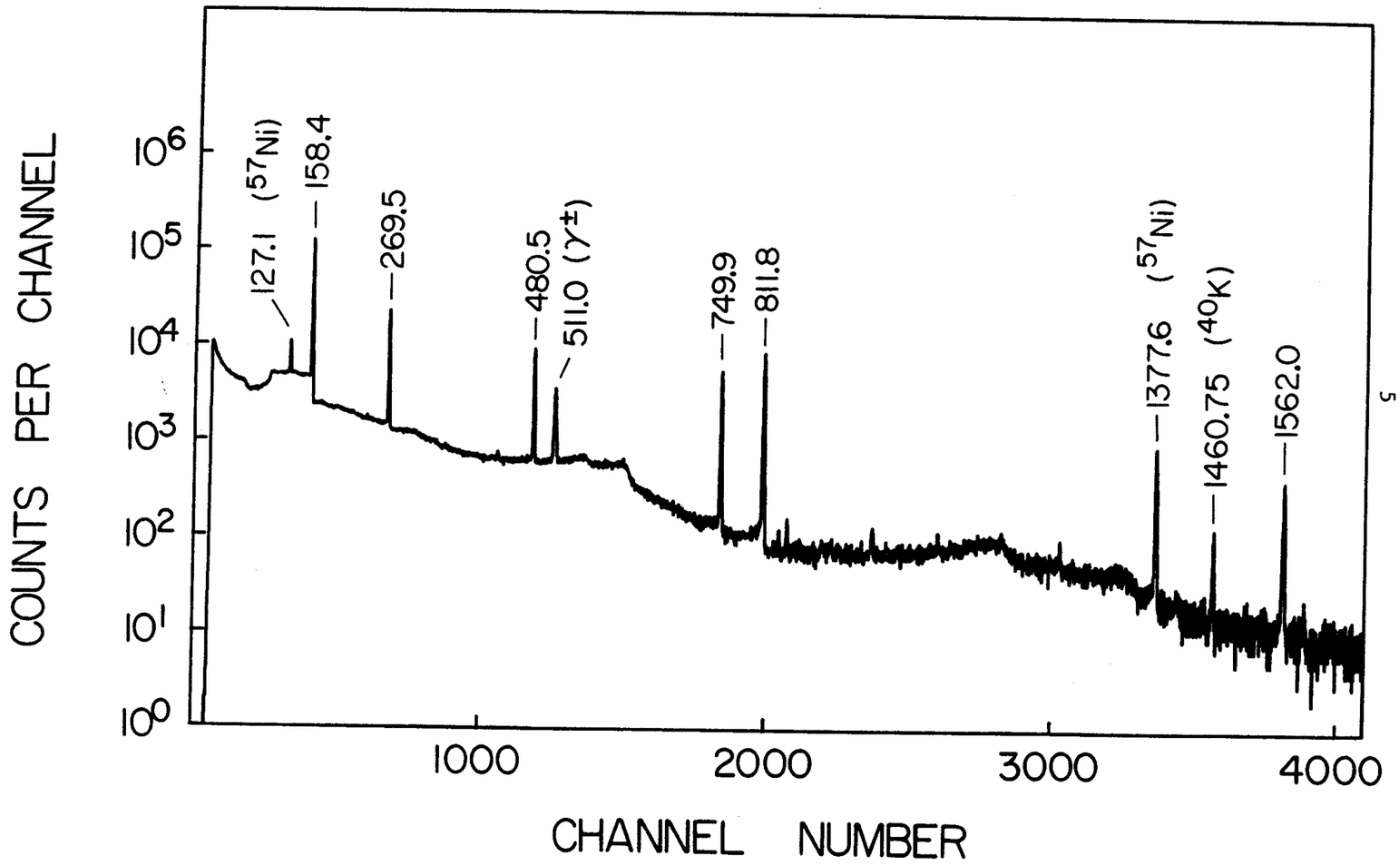

Figure 1. Typical ^{56}Ni singles spectrum taken with the 2.5% efficient Ge(Li) spectrometer.

peaks and the ^{56}Ni decay peaks grew into the spectra at roughly equal rates. A quadratic fit was then made to the calibration energies versus measured centroids in two energy regions (100-800 keV and 700-2000 keV). The ^{56}Co γ-ray energies were then calculated by computer using this calibration and are listed in Table I.

The 2.5%- and 10.4%-efficient Ge(Li) detectors were both used for γ-ray intensity determinations. Separate singles spectra were taken using each detector with the ^{56}Ni source placed both at 5 cm and at 25 cm from the face of the detector. The use of two detectors with highly different efficiencies and of two source-to-detector distances allowed for sum-peak identification. Background spectra (with the source removed) were also taken with each detector. The relative efficiency curves were determined using the γ-ray intensity standards ^{160}Tb, ^{203}Hg, ^{180m}Hf, ^{110m}Ag, ^{177m}Lu, ^{56}Co, ^{88}Y, ^{60}Co, and ^{24}Na. The relative intensities of the γ-rays from these standards can be found elsewhere.[5,37-39] The intensities presented in Table I were obtained by averaging the four sets of data.

Table I. Energies and relative intensities of the γ rays in ^{56}Co from the beta decay of ^{56}Ni.

E_γ (keV)		I_γ	
Present work	Piluso *et al.*[a]	Present work	Piluso *et al.*[b]
158.4±0.1	158.3±0.2	≡ 100.	≡ 100.
269.5±0.1	269.6±0.1	36.0±1.4	40.0±0.7
480.5±0.1	480.7±0.1	36.0±1.5	41.4±1.4
749.9±0.1	750.6±0.1	50.5±2.5	54.3±3.5
811.8±0.1	812.2±0.2	88.5±4.4	91.3±3.5
1562.0±0.2	1562.5±0.2	14.3±1.4	12.8±1.4

[a] See Ref. 4.

[b] The relative γ-ray intensities presented by Piluso *et al.* (Ref. 4) have been renormalized here to 100 for the intensity of the 158.4-keV transition.

C. γ-γ Coincidences

Prompt γ-ray coincidences in the ^{56}Ni beta decay were determined with a Ge(Li)-Ge(Li) spectrometer using the 4.5%- and 10.4%-efficient detectors arranged in 150° geometry with a graded (Pb-Sn-Cu) absorber placed between them to minimize Compton scattering from one detector into the other. A typical two-parameter, fast-slow coincidence arrangement (resolving time $2\tau \cong 100$ nsec) was used. Addresses corresponding to the energies of coincident γ-rays were listed in pairs on magnetic tape.[40] This listing yielded a 4096×4096-channel array of prompt coincidence events which were later sorted off-line in gated slices.[41] The gated slices included careful subtraction of background coincidences which were determined from the adjacent continuum.

The integral coincidence spectrum from each detector is shown at the top of Fig. 2. Each spectrum represents 330,000 coincidences. Beneath each integral spectrum in Fig. 2 are shown spectra in coincidence with the various ^{56}Co peaks. The results are summarized in Table II.

Figure 2. Integral coincidence and gated spectra from the ^{56}Ni γ-γ coincidence experiment. Peaks labeled with a Σ were identified as triple coincidences where two of the three coincident γ rays have been summed in one detector. Peaks labeled in parentheses are believed to be from chance coincidences or insufficient background subtraction.

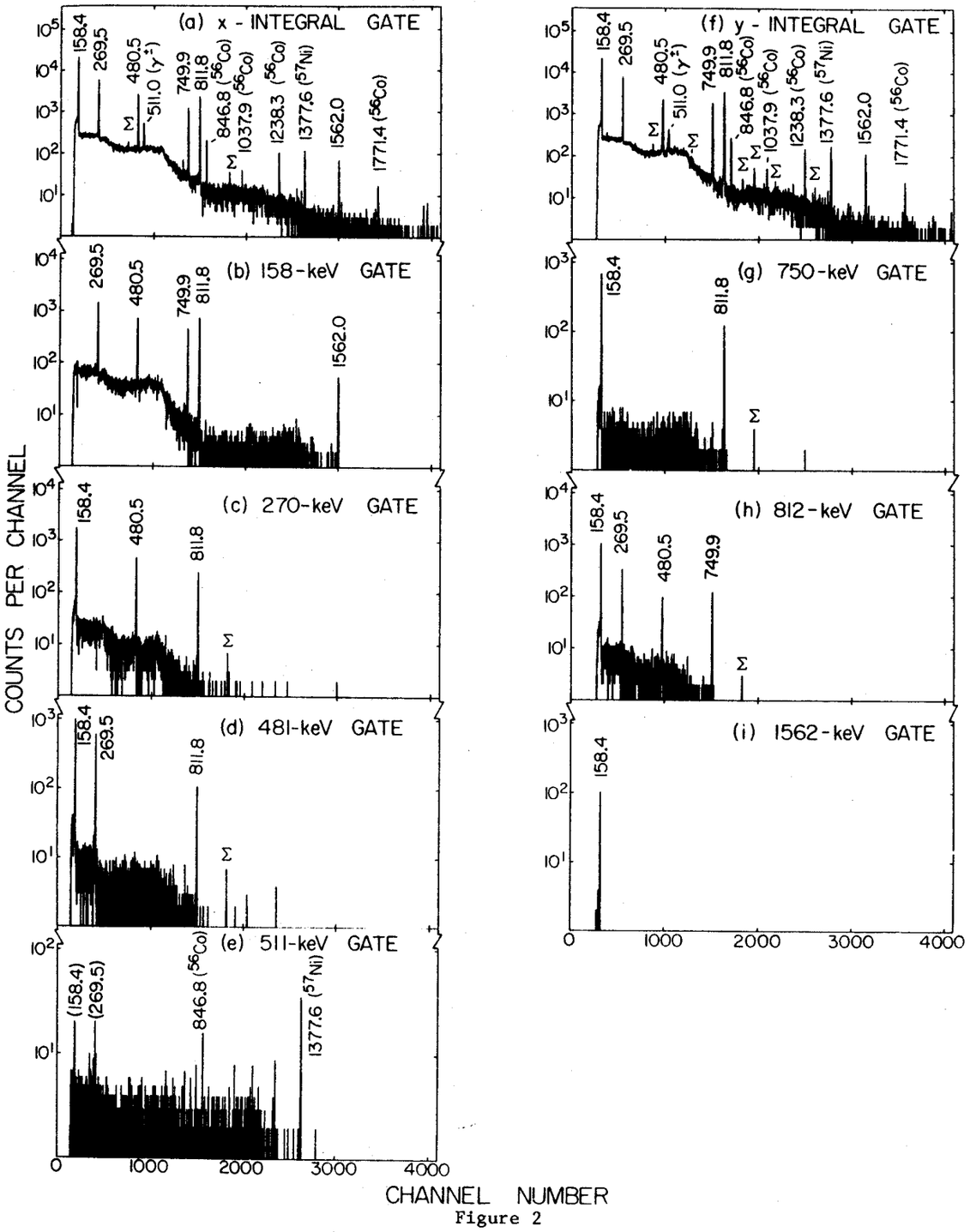
(a) x - INTEGRAL GATE
158.4
269.5
480.5
511.0 (γ±)
749.9
811.8
846.8 (56Co)
1037.9 (56Co)
1238.3 (56Co)
1377.6 (57Ni)
1562.0
1771.4 (56Co)
(b) 158-keV GATE
(c) 270-keV GATE
(d) 481-keV GATE
(e) 511-keV GATE
(158.4)
(269.5)
(f) y - INTEGRAL GATE
(g) 750-keV GATE
(h) 812-keV GATE
(i) 1562-keV GATE
COUNTS PER CHANNEL
CHANNEL NUMBER
0
1000
2000
3000
4000

Figure 2

Table II. Summary of two-parameter γ-γ coincidence results for the $^{56}Ni \xrightarrow{\epsilon} {}^{56}Co$ decay.

E_γ / E_γ (keV)	158	270	481	511($\gamma^{\pm}$)	750	812	1562
158	---	yes	yes	no	yes	yes	yes
270	yes	---	yes	no	no	yes	no
481	yes	yes	---	no	no	yes	no
511($\gamma^{\pm}$)	no	no	no	---	no	no	no
750	yes	no	no	no	---	yes	no
812	yes	yes	yes	no	yes	---	no
1562	yes	no	no	no	no	no	---